IRSTI 41.27.29, 89.51.17 https://doi.org/10.26577/phst.2020.v7.i2.02

Physical properties of dark matter in galaxy U11454

K. Boshkayev[1], T.K. Konysbayev[2], E.B. Kurmanov[2],
M. Muccino[3,*] and G. Zhumakhanova[1]

[1]*International Center for Relativistic Astrophysics, 10, Republic square, I–65122 Pescara, Italy*
[2]*School of Science and Technology, University of Camerino,*
16, Via Andrea D'Accorso, 62032, Camerino, Italy
[3]*National Institute of Nuclear Physics (INFN), National Laboratory of Frascati,*
54, Via Enrico Fermi, 00044 Frascati, Italy
[*]*e-mail: marco.muccino@lnf.infn.it*

In this paper physical characteristics of dark matter distribution in the spiral galaxy U11454 is explored using only well-known cored density profiles in the literature such as the pseudo-isothermal, Burkert, Einasto, exponential sphere, Beta and Brownstein profiles. It is presumed that the distribution of dark matter in the considered galaxy is spherically symmetric without taking into account its complex structural components. It is assumed that dark matter possesses non-vanishing pressure which allows theoretically analyzing the state parameter. The model free parameters of each profile are inferred from the rotation curve data of the galaxy by means of non-linear model fit procedure. Using the Bayesian Information Criterion the best fit profile among the considered ones is selected. Furthermore, the hydrostatic equilibrium equation is solved and the pressure profiles for each above mentioned density profile are constructed in the weak gravitational field regime. Combining the pressure and corresponding density profiles one gains equations of state for the dark matter in the galaxy U11454. The mass and gravitational potential are evaluated and constructed as a function of the radial distance for each profile. The total dark matter mass is assessed and our results are confronted and contrasted with the previous outcomes. In addition, the speed of sound is estimated in the dark matter distribution and it is shown that its behavior is quite unusual especially for the Brownstein profile. Finally, the refracting index is calculated in order to assess gravitational lensing effects produced by the presence of dark matter and astrophysical implications of the obtained results are discussed.

Key words: dark matter, rotational curves, equation of state, speed of sound and refractive index.
PACS number: 95.35.+d, 98.35.−a

1 Introduction

Dark matter (DM) interacts with ordinary matter via gravity. For this reason it is inaccessible to direct observations and measurements. Recent cosmological surveys have demonstrated that DM represents the 26.8 % of the total energy budget of the Universe [1]. So far, from a theoretical viewpoint it was assumed that DM consists of some experimentally undiscovered particles derived from the extension of the standard model of particle physics [2, 3].

Astronomers and astrophysicists indirectly receive all information about DM from rotation curves (RCs) of galaxies and gravitational lensing effects. RCs represent profiles of linear velocity $v(r)$ of stars and gas in circular orbits as functions of radial distance r from the galactic center to the outer parts. The RCs of galaxies have an amplitude that remains almost constant with increasing distance, even outside the stellar disk, which is not normally expected in Newtonian gravity (NG) [4, 5]. According to some studies it is presumed that the DM consists of nonrelativistic and collisionless particles, whose cross sections lie around $\sim 10^{-26}$ cm^2 [6].

In this work to study the distribution of DM in the chosen galaxy we mainly consider widely used density profiles such as: the pseudo-isothermal (ISO), Burkert, Beta, Brownstein, Einasto and exponential sphere in the framework of NG. By analyzing the RCs data points we derive the unknown model parameters of the DM halo for all profiles. In analogy to our previous work [7] we suppose that the DM equation of state (EoS) in a particular galaxy, by default, do not depend upon

the density profiles. Hence, we intend to check whether this assumption is valid or not for the galaxy U11454 as well. Moreover, to avoid the cuspy halo problem we mainly focus on the cored density profiles. This treatment is consistent with the fact that the DM density and pressure at the galactic center must be finite.

Following Ref. [7] we solve the hydrostatic equilibrium equation within NG to find the pressure profiles. The DM EoS for galaxy U11454 can be obtained by expressing pressure in terms of density for each individual model. For some profiles EoS is obtained analytically, but for others this can be done numerically only. Thus, the main objective of this work is to test whether the DM EoS depends on the adopted density profile or not. Using the DM EoS, we calculate the speed of sound and also the refractive index, which play a pivotal role in the formation of structures and in the gravitational lensing effect.

The paper is organized as follows. The DM phenomenological profiles and their characteristics are presented in section 2. The basic equation and their analytic solutions are displayed in section 3. The fitting methods of the observational data of U11454 RC and the major numerical results on the EoS, speed of sound and refractive index are rendered in section 4. Conclusions and perspectives of our work are summarized in section 5.

2 Phenomenological dark matter profiles

The distribution of DM in galaxies is not uniform, concentrating at their centers and dropping off at the periphery. Using the methods of numerical simulation of the dynamics of stars in galaxies, one can find the corresponding DM distribution function or its profile. In this paper, we have chosen traditionally used cored DM density profiles, such as the pseudo-isothermal, Beta, Burkert, Brownstein, Einasto and exponential sphere. All profiles that we used in this work are characterized by two parameters: the DM density at the centers of galaxies or the characteristic density ρ_0 and the scale radius r_0, except for the Einasto profile, which has one more free parameter.

Thus, we employ the following models:

1. The ISO profile [8]:

$$\rho_{Iso}(r) = \frac{\rho_0}{1+x^2}, \tag{1}$$

where $x = x(r) = r/r_0$, r is the radial coordinate/distance. The model depends upon the two constants r_0 and ρ_0, so do the following profiles.

2. Exponential sphere [9]:

$$\rho_{Exp}(r) = \rho_0 e^{-x}. \tag{2}$$

3. Burkert profile [10]:

$$\rho_{Bur}(r) = \frac{\rho_0}{(1+x)\left(1+x^2\right)}. \tag{3}$$

4. The Beta profile with $\beta = 1$ [11, 12]:

$$\rho_{Beta}(r) = \frac{\rho_0}{\left(1+x^2\right)^{3/2}}. \tag{4}$$

5. Brownstein profile [12, 13]:

$$\rho_{Bro}(r) = \frac{\rho_0}{1+x^3}. \tag{5}$$

6. Einasto profile [14]:

$$\rho_{Ein}(r) = \rho_0 \exp\left[2\alpha\left(1-x^{1/\alpha}\right)\right], \tag{6}$$

where α is the Einasto free parameter, which determines the slope of the profile [15].

In Figure 1 we illustrate the dependence of ρ/ρ_0 on r/r_0 for various phenomenological DM halo profiles. In this dimensionless representation the profiles depict diverse behavior especially at large distances. Note that ρ_0 and r_0 are different for each profile. The central density for the Einasto profile is determined as $\lim_{r\to 0}\rho_{Ein}(r) = \rho_0 e^{2\alpha}$.

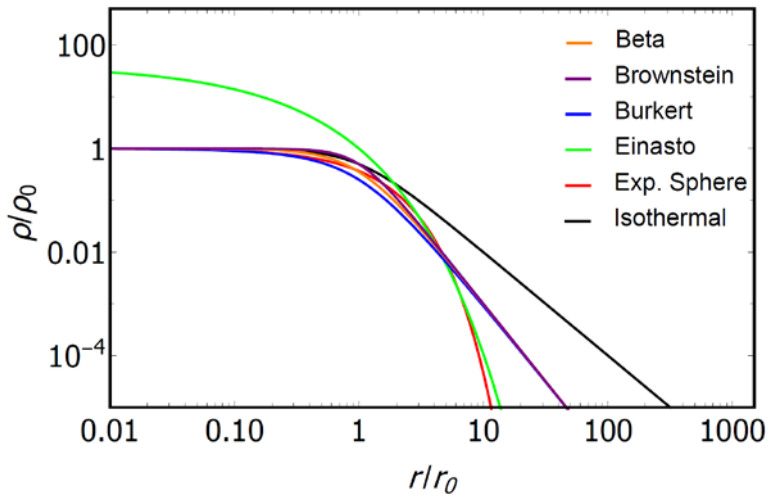

Figure 1 – Color online. Different phenomenological DM density profiles. For the Einasto profile we use $\alpha = 1.8$ inferred from the RC data points

3 Equations of hydrostatic equilibrium and analytic results

The main goal of this work is to obtain the equation of state of DM in the NG regime. To do so we start with the standard Newtonian hydrostatic equilibrium equations, given by [16, 17]

$$\frac{dM(r)}{dr} = 4\pi r^2 \rho(r), \tag{7}$$

$$\frac{dP(r)}{dr} = -\rho(r)\frac{GM(r)}{r^2}, \tag{8}$$

$$\frac{d\Phi(r)}{dr} = \frac{GM(r)}{r^2}, \tag{9}$$

where $M(r)$ is the mass profile enclosed inside the sphere of radius r, $P(r)$ is the DM pressure, G is the Newtonian gravitational constant and $\Phi(r)$ is the gravitational potential. To obtain expressions for the pressure the density profiles Eqs. (1) – (6) are separately plugged in Eqs. (7) – (8). We integrate the expression for the pressure, using boundary conditions, imposing that P vanishes as r approaches infinity and P becomes finite as r tends to zero.

For the ISO, Beta and exponential sphere profiles all calculations were performed analytically, whereas for the Einasto, Brownstein and Burkert profiles all analyzes were carried out numerically. The pressure and EoS formulas for the ISO and exponential sphere profiles in Eqs. (1) and (2) are given in Ref. [7], for the Beta profile we obtain the following equation

$$M_{Beta}(r) = 4\pi r_0^3 \rho_0 \left\{ \operatorname{arsinh}(x) - \frac{x}{\sqrt{1+x^2}} \right\}, \tag{10}$$

$$P_{Beta}(r) = 4\pi G r_0^2 \rho_0^2 \left\{ \frac{1}{2\left(1+x^2\right)} + \frac{1+2x^2}{x\sqrt{1+x^2}} \operatorname{arsinh}(x) - 2\ln\left(2\sqrt{1+x^2}\right) \right\}, \tag{11}$$

$$\Phi_{Beta}(r) = -\frac{4\pi G r_0^2 \rho_0}{x} \left\{ \operatorname{arsinh}(x) - \frac{x}{\sqrt{1+X^2}} \right\}, \tag{12}$$

where $x = r/r_0$ as before, $X = R/r_0$ and R is the radius of the DM halo, evaluated by matching interior and exterior potentials. Since R is not well-defined quantity, usually, for practical purposes one sets it equal to the virial radius of the DM halo.

3.1 Dark matter equation of state

The EoS of a given fluid characterizes the physical features of the fluid itself and shows how it develops when it is not in equilibrium. Combining Eq. (11) together with Eq. (4), we obtain the EoS for the Beta profile

$$P_{Beta}(\rho) = 4\pi G r_0^2 \rho_0^2 \left\{ \frac{\xi}{2} + \frac{2-\xi}{\sqrt{\xi-1}} \operatorname{arsinh}\left(\sqrt{\frac{\xi-1}{\xi}} \right) - 2\ln\left(\frac{2}{\sqrt{\xi}} \right) \right\}, \quad (13)$$

where $\xi = \xi(\rho) = (\rho/\rho_0)^{2/3}$. Eq. (13) for the Beta profile has been obtained here for the first time.

Furthermore, the thermodynamic properties of the fluid are hidden inside the state parameter defined by [18]

$$\omega = \frac{P}{c^2 \rho}, \quad (14)$$

which is also known as a baratropic parameter. In our case, the pressure does not vanish inside the DM distribution and the corresponding formulas for the EoS are complicated for some profiles.

3.2 Speed of sound and refractive index

Using the speed of sound c_s, we can account for perturbations caused by the DM fluid. Its definition in case of adiabatic perturbations is [19]

$$c_s^2 = \left(\frac{\partial P}{\partial \rho} \right)_S. \quad (15)$$

The speed of sound for the ISO and exponential sphere profiles are given in Ref. [7] and for the Beta profile we find it from Eq. (13)

$$c_{s(Beta)}^2 = \frac{4\pi G r_0^2 \rho_0}{3} \frac{\sqrt{\xi}}{1-\xi} \times \times \left\{ \frac{1}{\sqrt{1-\xi}} \operatorname{arsinh}\left(\sqrt{\frac{1-\xi}{\xi}} \right) - 1 \right\}. \quad (16)$$

Additionally, we calculate and show that DM gives a refractive index which is slightly larger than pure vacuum. This can be seen when studying the optical properties of the galaxy under consideration. Thus, we here examine the refractive index of DM halo of the galaxy U11454 for all adopted profiles. The refractive index in the field of DM in the weak field regime is given by [20]

$$n(r) = 1 - \frac{\Phi(r)}{c^2} - \int \frac{GM(r)}{c^2 r^2} dr, \quad (17)$$

where $\Phi(r)$ is the internal gravitational potential for a given DM density profile, obtained by solving Eq. (9) and c is the speed of light in vacuum. The integration is carried out within the range of the radial coordinate taken from the RC data points.

4 Methods, analyses and numerical results

We aim to show that as a result of our analysis, by testing different profiles for such a galaxy, DM halo density law can be accounted for the kinematics of the whole family of disk (spiral) galaxies like U11454. For completeness, it is important to stress that the contributions of gas in the bulge and disk of the galaxy are crucial to characterize the RCs. In turn, the RC allows one to determine the distribution of the galaxy's mass along the radial distance. In the standard approach, all the constituents of the galaxy must be accounted for in analogy with Ref. [9]. However their contributions with respect to the DM halo are small. Moreover the inner parts of U11454 is not fully reported in the literature. Therefore, one can neglect the contribution of all the constituents of the galaxy, apart from the halo, for simplicity and adopt

$$\upsilon_{tot}^2 \simeq \upsilon_{profile}^2, \quad (18)$$

where $\upsilon_{profile}$ is the contributions of the DM halo profile velocity. So, $\upsilon_{profile}$ is defined by

$$\upsilon_{profile} = \upsilon(r) = \sqrt{\frac{GM(r)}{r}} \text{ and}$$

$$M(r) = \int_0^r 4\pi r^2 \rho(r) dr, \qquad (19)$$

where the DM mass $M(r)$ has been obtained by integrating Eq. (7), exploiting Eqs. (1) – (6).

Further, we apply the Levenberg-Marquardt nonlinear least squares method [21, 22] to find the minimum of the χ^2 function. The Levenberg-Marquardt algorithm is an iterative technique that locates the minimum of a function which is expressed as the sum of squares of nonlinear functions. It consists in a combination of the Gauss–Newton algorithm and the method of the steepest descent gradient. So, the χ^2 function is defined by

$$\chi^2 = \sum_{i=1}^{N} \left[\frac{\upsilon_i^{obs} - \upsilon(\rho_0, r_0, r)}{\sigma_{\upsilon,i}^{obs}} \right]^2, \qquad (20)$$

where υ_i^{obs} and $\sigma_{\upsilon,i}^{obs}$ are the N data points of U11454 RC and their corresponding errors, respectively (see Fig. 2, Left panel), while $\upsilon(\rho_0, r_0, r)$ is given by Eq. (19) and describes the RCs for each DM profile. The best fit parameters, minimizing the χ^2 for each DM profile are listed in Table 1 and shown in Figure 2 (Left panel). The ρ_0 and r_0 parameters listed in Table 1 are in agreement with the results of Ref. [23]. The amount of DM mass in the galaxy, computed by using different profiles, is also shown in Table 1 and it is shown to be consistent with the results of Ref. [23] for the ISO and Burkert profiles. The χ^2 values are also shown in the last column of Table 1.

Table 1 – Model parameters for galaxy U11454. We report for each profile ρ_0, r_0 and the masses expressed in units of solar mass $M_\odot$ with their error bars, respectively. The last two columns present the BIC statistical outputs and corresponding chi squares used for computing the BIC values. r_{vir} denotes the virial radius determined as the radius at which the density is equal to the critical density of the Universe multiplied by 200 and M_{vir} is the corresponding virial mass. [a] DM mass is calculated using the last data point in the halo for r. [b]DM mass is calculated using the scale radius r_0. [c]The values $\text{BIC} \equiv \{84, 91, 79, 76, 85, 67\}$ are for the Beta, Brownstein, Burkert, Einasto, exponential sphere and ISO, respectively; we define $\Delta\text{BIC} \equiv \text{BIC} - \text{BIC}_0$, with $\text{BIC}_0 = 67$ the Isothermal reference value. For the Einasto profile $\alpha = 1.8 \pm 0.3$.

Profiles	$\rho_0 \pm \sigma_{\rho_0}$, ($10^{-3}\ M_\odot/pc^3$)	$r_0 \pm \sigma_{r_0}$ (kpc)	r_{vir}, (kpc)	M_{vir}, ($10^{10}\ M_\odot$)	$M \pm \sigma_M$ [a], ($10^{10}\ M_\odot$)	$M \pm \sigma_M$ [b], ($10^{10}\ M_\odot$)	ΔBIC[c]	χ^2
Beta	104.0 ± 10.8	3.7 ± 0.2	56.8	15.6	6.0 ± 1.0	1.1 ± 0.3	17	1.5
Brownstein	81.0 ± 10.0	3.6 ± 0.3	51.7	12.7	5.7 ± 1.2	1.1 ± 0.4	24	2.8
Burkert	139.0 ± 12.9	3.7 ± 0.2	62.3	18.6	6.1 ± 0.9	1.1 ± 0.3	12	1.0
Einasto	10.5 ± 2.6	7.2 ± 0.9	42.5	14.0	6.4 ± 2.2	3.4 ± 2.0	9	0
Exp. Sphere	130.9 ± 12.9	2.8 ± 0.2	24.1	7.5	5.9 ± 1.0	0.6. ± 0.2	18	1.7
ISO	151.0 ± 11.7	1.9 ± 0.1	142.8	98.6	6.5 ± 0.8	0.3 ± 0.1	0	0.4

To compare the selected 6 profiles, which have different number of parameters and are not nested into each other, we employ the Bayesian Information Criterion (BIC) [24]. BIC is a selection criterion among a finite set of models, conceived to solve the overfitting issue when increasing the number of parameters in the fitting function. For completeness, notice that other selection criteria could also be used, e.g. the Akaike information and/or DIC criteria [25, 26]. Starting from the χ^2 definition, the BIC is defined as

$$\text{BIC} = \chi^2 + k \ln \text{N}, \qquad (21)$$

where k is the number of model parameters. For the Einasto profile $k = 3$, while for all the other profiles $k = 2$. A profile with a minimum BIC value is favored, according to Ref. [27]. As one can see from Table 1 for galaxy U11454 the BIC value is minimum for the ISO profile and is maximum for the Brownstein profile, though the difference between the values is not large.

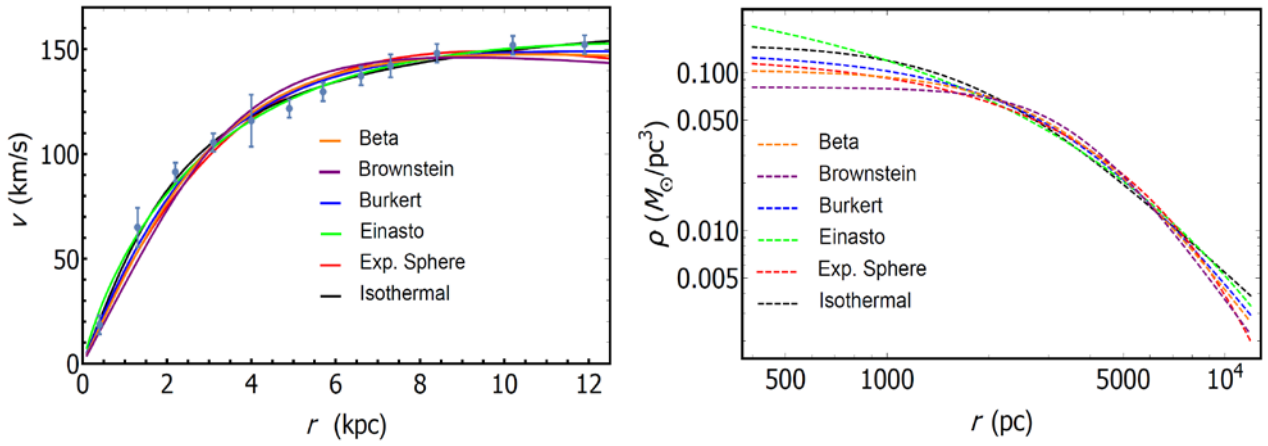

Figure 2 – Color online. Left panel: RC of galaxy U11454 and fitted profiles. Right panel: Logarithmic density profiles of DM in the halo.

In Figure 2 (Left panel) we construct RC of galaxy U11454 and theoretical curves for different profiles adopted in this work. Here the gray thick points show the observational data with their error bars, solid curves show fitted ISO (black), exponential sphere (red), Einasto (green), Burkert (blue), Beta (orange) and Brownstein (purple) profiles. In the Right panel we present the density profiles with inferred model parameters from the fit.

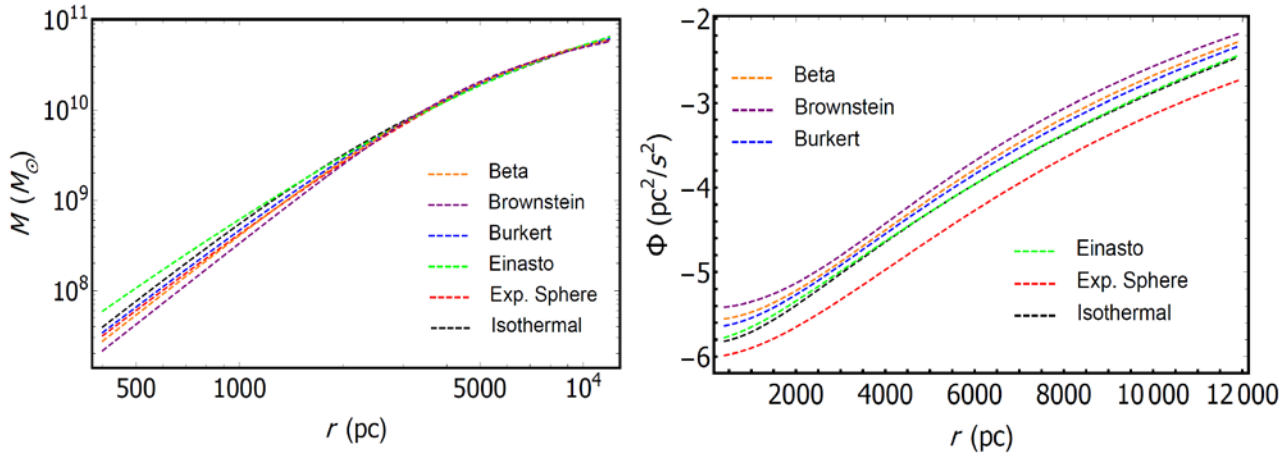

Figure 3 – Color online. Left panel: Logarithmic mass profiles of DM in the halo. Right panel: Logarithmic gravitational potential of DM in the halo. Note that $\Phi(r)$ is multiplied by 10^{-23}

In Figure 3 the mass in units of solar mass is plotted as a function of the radial coordinate (Left panel). At large distances all profiles produce similar mass. Correspondingly, the internal gravitational potential is illustrated as a function of the radial coordinate in the considered range (Right panel). The behavior of the potential for various profiles is almost identical.

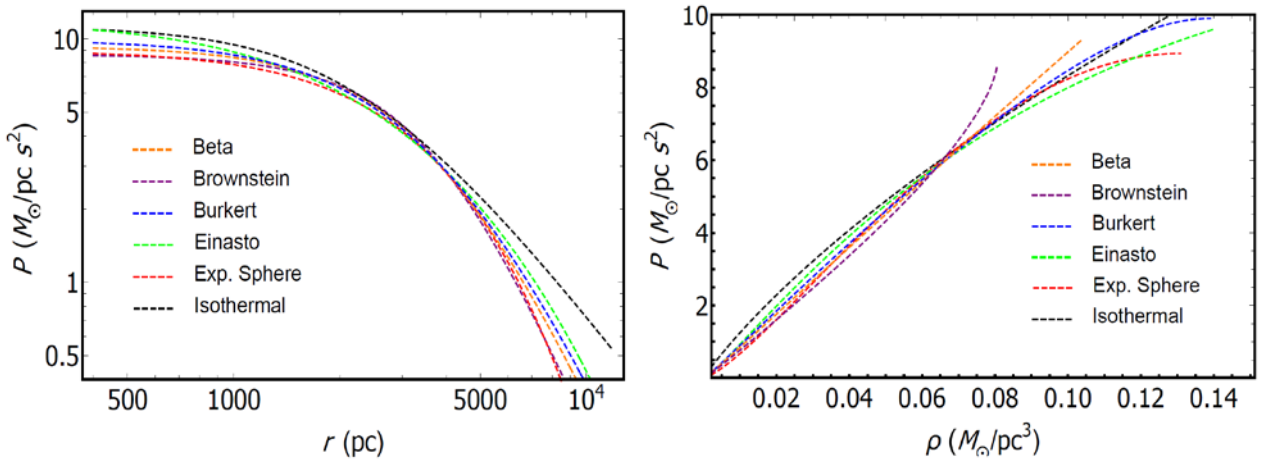

Figure 4 – Color online. Left panel: Logarithmic pressure profiles of DM in the halo. Right panel: The equation of state of DM halo. Note that P in both panels is multiplied by 10^{-25}

In Figure 4 we plotted the pressure profiles $P(r)$ (Left panel) and equation of state $P(\rho)$ (Right panel) for galaxy U11454, using all the DM halo models i.e. Eqs. (1) – (6), by solving Eqs. (7) – (8). Here one can choose different units by using the following conversion factors for the density and pressure:

$$1\mathrm{M}_\odot/\mathrm{pc}^3 = \\ = 6.77\times10^{-23}\,\mathrm{g}/\mathrm{cm}^3 = \\ = 38.05\left(\mathrm{GeV}/c^2\right)/\mathrm{cm}^3$$

and

$$1\mathrm{M}_\odot/(\mathrm{pc\,s}^2) = \\ = 6.44\times10^{14}\,\mathrm{g}/\left(\mathrm{cm\,s}^2\right) = \\ = 3.62\times10^{38}\left(\mathrm{GeV}/c^2\right)/\left(\mathrm{cm\,s}^2\right),$$

respectively.

It is fascinating to study the general behavior of the EoS involving the state parameter ω. Consequently, (14) can be written either in terms of the radial coordinate r or density ρ, as shown in Figure 5. It follows that ω tends to zero for large distances or low densities, except for the ISO profile, where it becomes constant. At small distances or high densities, ω decreases or tends to a constant value, except for the Brownstein profile which grows in an unusual manner, at least in the considered range of distances provided by the RC data points.

In our calculations, we can also take into account the corrections provided by general theory of relativity. At large distances when $\rho << \rho 0$ the corrections can be neglected. However, near the central part of the galaxy, its deviations from NG would be significantly noticeable, since the corrections of general relativity in pressure are clearly much larger than in NG [28]. This is simply a consequence of the Tolman-Oppenheimer-Volkov system of equations.

Besides, in Figure 6 (Left panel) we plotted the speed of sound according to Eq. (15) for all the profiles. An unusual feature of DM is the fact that with increasing density, the speed of sound decreases for all profiles apart from the Brownstein profile where the opposite is true. It is known from cosmology that if the speed of sound in the central part of the DM distribution is less than in its outer parts, then it allows the formation of large-scale structures [29]. Thus, we can say and state that the Brownstein profile is not appropriate to form galaxies. Hence, one can rule it out.

It should be recalled that for the ISO, exponential sphere, Burkert, Beta and Brownstein profiles ρ_0 is the central density. However for the Einasto profile ρ_0 is the characteristic density and its central density is equal to $\rho_0 e^{2\alpha}$ as indicated above. As can be seen from Fig. 6 (Left panel), the behaviors of the curves for the speed of sound are very different, some of them change drastically as a function of the density. Our results are similar to the ones of Ref. [30], but for another galaxy.

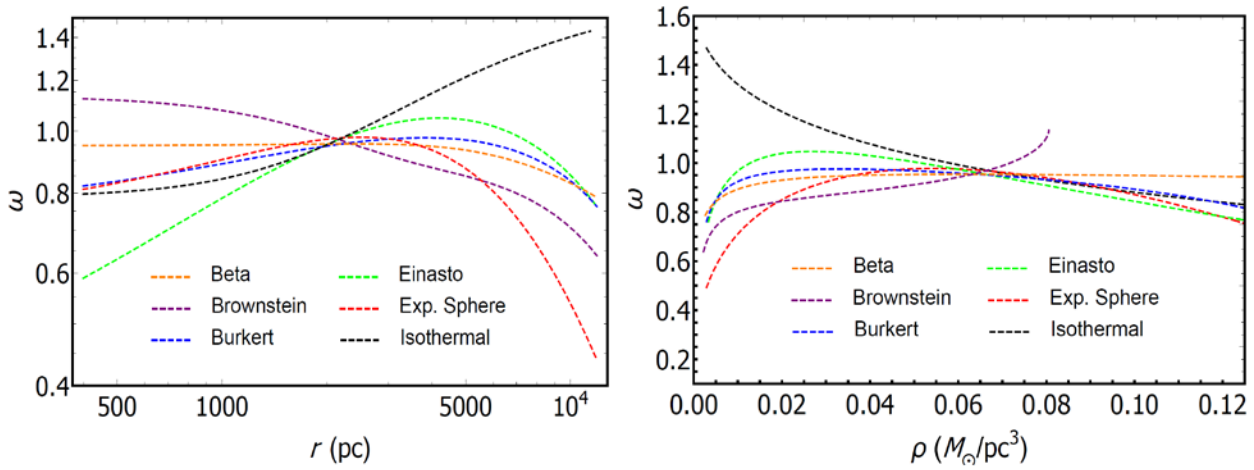

Figure 5 – Color online. Left panel: Dimensionless state parameter ω as a function of radial coordinate r. Right panel: Dimensionless state parameter ω as a function of density ρ. Note that ω in both panels is multiplied by 10^{-7}

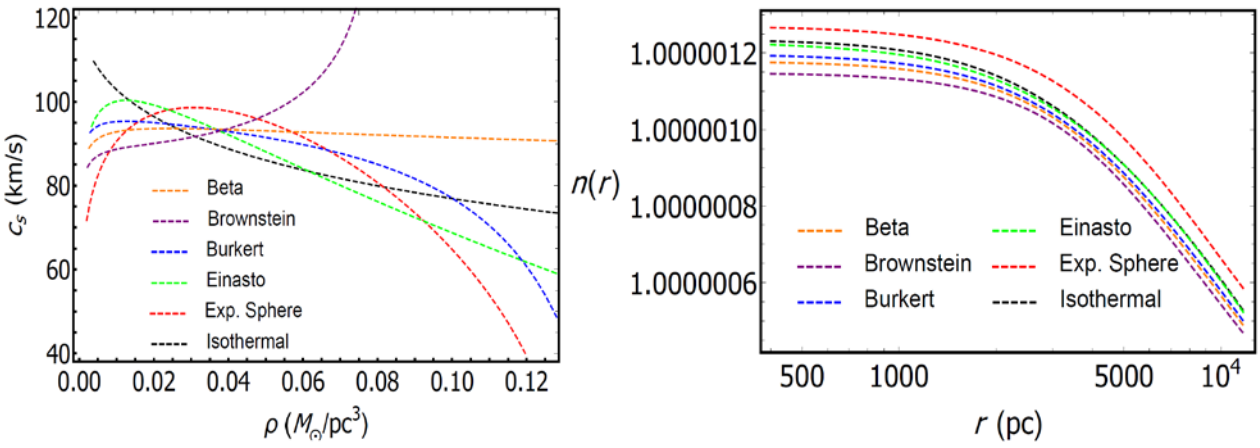

Figure 6 – Color online. Left panel: The speed of sound in the DM distribution for different profiles. Right panel: The refractive index for DM in galaxy U11454.

For the above considered profiles we have shown the dependence of the refractive index n on the radial coordinate in the DM distribution in Fig. (6) (Right panel). The value of the refractive index is small in the halo, as we expected. In the disk region the refractive index grows up slowly to the direction of the galactic center. In the core region the refractive index becomes almost constant. The overall change in the refractive index is extremely small, less than 1 part of 10^6. The refractive index in vacuum is slightly less than in DM for all the profiles that we used at a distance within

(0.4 – 11.9) kpc which corresponds to the RCs data points. In general, the refractive index can also be used to study the light propagation process in the epoch of DM dominance [31].

5 Conclusion

By analyzing the RC data points of the fuzzy spiral galaxy U11454, we inferred the free parameters of the models with the help of the least squares method. We used the well-known cored DM density profiles from the literature and, in addition, we considered the exponential sphere, Beta and Brownstein profiles for comparison. The exponential sphere profile is usually applied to study the inner parts of galaxies [9] and, in fact, for galaxy

U11454 it showed a good result. This can be seen from Table 1.

Out of all the considered profiles, the Brownstein profile has the highest BIC value, and the ISO profile has the lowest value. The same is true also for the χ^2. The difference in the BIC between ISO profile (with the smallest value) and Brownstein profile (with the highest value) is $\Delta\mathrm{BIC} = 24$ and exhibits very strong evidence against the Brownstein profile. Among other profiles, the only one with the least evidence against it, though still strong, is the Einasto profile with $\Delta\mathrm{BIC} = 9$. So, for our purposes the ISO and Einasto profiles are the most convenient profiles to study the DM EoS of the galaxy U11454.

Inspecting the curves for $\rho(r)$, $P(r)$ and $P(\rho)$, we have seen that the behavior of the profiles is similar to each other, but the degeneracy among the profiles is completely broken by looking at the diagram of the speed of sound. Here all profiles are distinct. As can be seen in Fig. 6 (Left panel), the speed of sound for the Brownstein profile behaves completely differently and does not allow to form structures.

Moreover we calculated the virial radius and corresponding mass. For that we used the condition when the density is equal to the critical density $\rho_{crit} = 9.31\times10^{-30}\,\mathrm{g/cm^3}$ [32] of the Universe multiplied by 200. The virial radius and corresponding mass turned out to be larger than the size of the galaxy inferred from the RC. Among the considered models the Isothermal profile produced the largest and the exponential sphere profile produced the smallest virial radius and corresponding mass.

In conclusion our analyzes demonstrate that for the considered galaxy the Isothermal, Einasto and Burkert profiles are the best models as they have the smaller BICs than the exponential sphere, Beta and Brownstein profiles. In accordance to our recent findings [7, 33, 34] the assumption that the EoS of DM do not depend on the model turned out to be partially valid only in a limited range of densities.

The features of DM such as the equation of state (the state parameter), refractive index and sound speed depend on the adopted models. If for the equation of state and refractive index the differences are extremely small, however for the sound speed the differences are quite noticeable. Therefore to explore the nature of DM one should attentively analyze DM profiles, accurately assess the value of BIC and rigorously examine the behavior of the sound speed. It would be also interesting to continue studies in this direction including contributions from the gas and disk, taking into account a composite structure of the galaxy. This issue will be addressed in our future works.

Acknowledgements. The work was supported by the Ministry of Education and Science of the Republic of Kazakhstan Grant: IRN AP08052311.

References

1. Planck Collaboration, Ade P.A.R. e.a.P.C. Planck 2013 results. I. Overview of products and scientific results // Astronomy and Astrophysics. – 2014. – Vol. 571. – A1.
2. Bertone G., Hooper D., Silk J. Particle dark matter: evidence, candidates and constraints // Physics Reports. – 2005. – V. 405. – P. 279-390.
3. Schumann M. Direct detection of WIMP dark matter: concepts and status // Journal of Physics G: Nuclear and Particle Physics. – 2019. – Vol. 46. – P. 103003.
4. Einasto J., Kaasik A., Saar E. Dynamic evidence on massive coronas of galaxies // Nature. – 1974. – Vol. 250. – P. 309–310.
5. Rubin V.C., Burstein D., Ford W. K. J., Thonnard N., Rotation velocities of 16 SA galaxies and a comparison of Sa, SB and SC rotation properties // Astrophysical Journal. – 1985. – Vol. 289. – P. 81–104.
6. Jungman G., Kamionkowski M., Griest K., Supersymmetric dark matter // Physics Reports. – 1996. – Vol. 267. – P. 195–373.
7. Boshkayev K., Konysbayev T., Kurmanov E., Luongo O., Muccino M. Imprint of Pressure on characteristic dark matter profiles: The case of ESO0140040 // Galaxies. – 2020. – Vol. 8. – P. 74.
8. Jimenez R., Verde L., Oh S.P. Dark halo properties from rotation curves // Monthly Notices of the Royal Astronomical Society. – 2003 – Vol. 339. – P. 243–259.
9. Sofue Y. Rotation curve and mass distribution in the galactic center – from black hole to entire galaxy // Publications of the Astronomical Society of Japan. – 2013 – Vol. 65. – P. 118.

10. Burkert A. The structure of dark matter halos in dwarf galaxies // The strophysical Journal Letters. – 1995 – Vol. 447. – L25–L28.

11. Navarro J.F., Frenk C.S., White S.D.M. Simulations of X-ray clusters // Monthly Notices of the Royal Astronomical Society. – 1995 – Vol. 275. – P. 720–740.

12. Sofue Y. Rotation curve of the Milky Way and the dark matter density // Galaxies. – 2020 – Vol. 8. – P. 37.

13. Brownstein J.R., Moffat J.W. Galaxy rotation curves without nonbaryonic dark matter // The Astrophysical Journal. – 2006 – Vol. 636. – P. 721–741.

14. Merritt D., Graham A.W., Moore B., Diemand J., Terzic B. Empirical models for dark matter halos. I. Nonparametric construction of density profiles and comparison with parametric models // The Astronomical Journal. – 2006 – Vol. 132. – P. 2685–2700.

15. Einasto J. On the construction of a composite model for the galaxy and on the determination of the system of galactic parameters // Trudy Astrofizicheskogo Instituta Alma-Ata. – 1965 – Vol. 5. – P. 87–100.

16. Shapiro S.L., Teukolsky S.A. Black holes, white dwarfs and neutron stars: The physics of compact objects. Wiley-VCH, 1986.

17. Misner C.W., Thorne K.S., Wheeler J.A. Gravitation. W. H. Freeman & Company: San Francisco, 1977.

18. Capozziello S., De Laurentis M., Luongo O., Ruggeri A. Cosmographic constraints and cosmic fluids // Galaxies. – 2013 – Vol. 1. – P. 216-260.

19. Capozziello S., D'Agostino R., Luongo O. Extended gravity cosmography // International Journal of Modern Physics D. – 2019 – Vol. 28. – P. 1930016.

20. Perlick V. Gravitational lensing from a spacetime perspective // Living Reviews in Relativity. – 2004 – Vol. 7. – P. 9.

21. Levenberg K. A method for the solution of certain non-linear problems in least squares // Quarterly of Applied Mathematics. – 1944 – Vol. 2. – P. 164–168.

22. Marquardt D. An algorithm for least-squares estimation of nonlinear parameters // Journal on applied mathematics. – 1963 – Vol. 11. – P. 431–441.

23. Garcia-Aspeitia M.A., Lopez-Dominguez J.C., Ortiz C. Hinojosa-Ruiz S., Rodriguez-Meza M.A. Energy density profile inspired by noncommutativity // Revista mexicana de física. – 2017– Vol. 63. – P. 423-438.

24. Schwarz G. D. Estimating the Dimension of a Model // Annals of Statistics. – 1963 – Vol. 6. – P. 461–464.

25. Akaike, H. A new look at the statistical model identification // IEEE Transactions on Automatic Control. – 1974 – Vol. 19. – P. 716–723.

26. Kunz M., Trotta R., Parkinson D.R., Measuring the effective complexity of cosmological models // Physical Review D. – 2006 – Vol. 74. – P. 023503.

27. Siutsou I., Argüelles C.R., Ruffini R. Dark matter massive fermions and Einasto profiles in galactic haloes // Astronomy Reports. – 2015 – Vol. 59. – P. 656–666.

28. Will C.M., The Confrontation between General Relativity and Experiment // Living Reviews in Relativity. – 2014 – Vol. 17. – P. 4.

29. Del Popolo A. Dark matter, density perturbations, and structure formation // Astronomy Reports. – 2007 – Vol. 51. – P. 169–196.

30. Barranco J., Bernal A., Núñez D. Dark matter equation of state from rotational curves of galaxies // Monthly Notices of the Royal Astronomical Society. – 2015 – Vol. 449. – P. 403–413.

31. Chechin, L.M., Kurmanov E.B., Konysbaev T.K. Geometrical Optics in a Universe with Dominance of Dark Matter // Russian Physics Journal. – 2020 – Vol. 63. – P. 58–63.

32. Di Paolo C., Salucci P., Erkurt A. The universal rotation curve of low surface between galaxies – IV.The interrelation between dark and luminous matter // Monthly Notices of the Royal Astronomical Society. – 2019. – Vol. 490. – P.5451 – 5477

33. Boshkayev K., Zhumakhanova G., Mutalipova K., Muccino M. Investigation of different dark matter profiles // News of the National Academy of Sciences of the Republic of Kazakhstan, Physico-Mathematical Series. – 2019. – Vol. 6. – No. 328. – P. 25 – 33.

34. Boshkayev K., Konysbayev T.K., Kurmanov E.B., Muccino M. Dark matter properties in galaxy U5750 // News of the National Academy of Sciences of the Republic of Kazakhstan, Physico-Mathematical Series. – 2020. – Vol. 6. – No. 334. – P. 81 – 90.